Environmental Toxicology and Pharmacology 94 (2022) 103913

Contents lists available at ScienceDirect

Environmental Toxicology and Pharmacology

journal homepage: www.elsevier.com/locate/etap

Developmental exposure to real-life environmental chemical mixture programs a testicular dysgenesis syndrome-like phenotype in prepubertal lambs

Chris S. Elcombe [a,b,**,1], Ana Monteiro [a,2], Matthew R. Elcombe [c,3], Mohammad Ghasemzadeh-Hasankolaei [a,4], Kevin D. Sinclair [d,5], Richard Lea [d,6], Vasantha Padmanabhan [e,7], Neil P. Evans [a,8], Michelle Bellingham [b,*,9]

[a] Institute of Biodiversity Animal Health and Comparative Medicine, College of Medical, Veterinary and Life Sciences, University of Glasgow, UK
[b] School of Veterinary Medicine, College of Medical, Veterinary and Life Sciences, University of Glasgow, UK
[c] MicroMatrices Associates Ltd, Dundee Technopole, James Lindsay Place, Dundee, UK
[d] University of Nottingham, Sutton Bonington Campus, Loughborough, UK
[e] Department of Pediatrics, University of Michigan, Ann Arbor, MI, USA

ARTICLE INFO

Edited by: M.D. Coleman

Keywords:
Developmental toxicity
Reproductive toxicity
Environmental chemicals
Testicular dysgenesis syndrome
Hypoxia inducible factor 1 alpha

ABSTRACT

Current declines in male reproductive health may, in part, be driven by anthropogenic environmental chemical (EC) exposure. Using a biosolids treated pasture (BTP) sheep model, this study examined the effects of gestational exposure to a translationally relevant EC mixture. Testes of 8-week-old ram lambs from mothers exposed to BTP during pregnancy contained fewer germ cells and had a greater proportion of Sertoli-cell-only seminiferous tubules. This concurs with previous published data from fetuses and neonatal lambs from mothers exposed to BTP. Comparison between the testicular transcriptome of biosolids lambs and human testicular dysgenesis syndrome (TDS) patients indicated common changes in genes involved in apoptotic and mTOR signalling. Gene expression data and immunohistochemistry indicated increased HIF1α activation and nuclear localisation in Leydig cells of BTP exposed animals. As HIF1α is reported to disrupt testosterone synthesis, these results provide a potential mechanism for the pathogenesis of this testicular phenotype, and TDS in humans.

1. Introduction

Male reproductive health has been in decline for the past 80 years (Carlsen et al., 1993). Reports indicate reduced fecundity, semen quality and serum testosterone concentrations, and increased incidence of reproductive disorders (cryptorchidism, hypospadias, hypogonadism,

Abbreviations: B, Biosolids; BTP, Biosolids treated pasture; BPA, Bisphenol A; BTB, Blood-testes barrier; C, Control; DGE, Differential gene expression; DEGs, Differentially expressed genes; EDCs, Endocrine disrupting chemicals; ECs, Environmental chemicals; FDR, False discovery rate; GO, Gene ontology; GD, Gestation Day; HIF1α, Hypoxia Inducible Factor 1 Alpha; PPCPs, Pharmaceuticals and personal care products; PBDEs, Polybrominated diphenyl ethers; PCBs, Polychlorinated biphenyls; PAHs, Polycyclic aromatic hydrocarbons; SCO, Sertoli-cell-only; TDS, Testicular dysgenesis syndrome; TDI, Tolerable daily intake.

* Correspondence to: University of Glasgow, Room 242, Jarrett Building, Garscube Estate, G61 1QH, Scotland.
** Correspondence to: University of Glasgow, Room 234D, Jarrett Building, Garscube Estate, , G61 1QH, Scotland.
E-mail addresses: Chris.Elcombe@glasgow.ac.uk (C.S. Elcombe), Michelle.Bellingham@glasgow.ac.uk (M. Bellingham).
[1] (0000-0002-7869-0123)
[2] (0000-0003-2349-9716)
[3] (0000-0003-3512-5025)
[4] (0000-0003-2053-5566)
[5] (0000-0002-6375-215X)
[6] (0000-0002-6793-3601)
[7] (0000-0002-8443-7212)
[8] (0000-0001-7395-3222)
[9] (0000-0002-3646-8989)

https://doi.org/10.1016/j.etap.2022.103913
Received 9 April 2022; Received in revised form 15 June 2022; Accepted 17 June 2022
Available online 20 June 2022

infertility, and testicular germ cell cancer), collectively known as testicular dysgenesis syndrome (TDS) (Sharpe and Skakkebaek, 2008; Skakkebæk et al., 2001). While many contributory factors to the decline in male fertility have been identified, including malnutrition, sedentary lifestyle, and stress, attention has focused on the role of environmental chemicals (ECs) (Crean and Senior, 2019; Ilacqua et al., 2018; Skakkebæk, 2002). Of the many ECs to which humans are routinely exposed, most attention is targeted at endocrine disrupting chemicals (EDCs), to which human epidemiological investigations provide links between fetal anti-androgenic EDC exposure and reduced male reproductive health (Rodprasert et al., 2021). A variety of ECs are known to adversely affect testicular development; for example, gestational exposure to phthalates is associated with negative effects on germ cell development, sperm motility, and testosterone production in rodents and humans (Borch et al., 2006; Hu et al., 2009). In addition to studies which have examined the effects of individual ECs, several rodent studies have used component-based methodologies to examine the effects of low dose mixtures of ECs. When presented as mixtures, adverse effects of EC exposure have been reported even when individual chemicals were present at doses at or below their respective tolerable daily intake (TDI) values (Buñay et al., 2018; Kortenkamp, 2014). This type of EC exposure scenario is of note as it more realistically reflects human EC exposure, which is characterised as chronic, extremely complex, and very low-level. However, it is not possible to accurately simulate true human EC exposure using component-based methodologies.

Solids from wastewater treatment, biosolids, are extensively used as an agricultural fertiliser and reflect human EC exposure in terms of complexity and concentration (Rhind et al., 2010, 2002, 2013; Venkatesan and Halden, 2014a, 2014b). When sheep are grazed on biosolids treated pasture (BTP), ECs can be measured in maternal tissues (Bellingham et al., 2012; Filis et al., 2019; Rhind et al., 2010, 2009, 2005), as well as tissues collected from their offspring (Rhind et al., 2010, 2009, 2005). Measured ECs include alkylated phenols, dioxin-like compounds, flame retardants such as polychlorinated biphenyls (PCBs) and polybrominated diphenyl ethers (PBDEs), pharmaceuticals and personal care products (PPCPs), plasticising agents such as phthalates and bisphenol A (BPA), polycyclic aromatic hydrocarbons (PAHs), and metabolites thereof (Rhind et al., 2002, 2013; Venkatesan and Halden, 2014a). Therefore, the BTP exposed sheep model is an appropriate model for investigation of the effects of generic human exposure to several different types of EC in parallel. Experiments using the BTP exposed sheep model have previously shown that *in utero* EC exposure can cause a multitude of effects in offspring. These include altered behaviour, differences in bone composition, disruption to cellular and hormonal processes, and changes in liver function, as well as effects on gonadal development in males and females (Bellingham et al., 2016, 2013, 2012, 2009; Elcombe et al., 2021; Erhard and Rhind, 2004; Filis et al., 2019; Fowler et al., 2008; Hombach-Klonisch et al., 2013; Lea et al., 2016, 2022; Lind et al., 2009; Paul et al., 2005). With specific regards to male gonadal development, gestational exposure to BTPs is associated with reduced testicular weight and fewer gonocytes, Leydig cells, and Sertoli cells in fetuses at gestation day (GD) 110 (Paul et al., 2005). Exposure to BTPs through maternal grazing from GD60 - GD140 is associated with reduced fetal mass, testes weight and adrenal weight, shorter anogenital distances, and reduced testosterone in GD140 fetuses (Lea et al., 2022). Of note is that these largely anti-androgenic effects parallel similar observations in the human (Rodprasert et al., 2021). In neonatal (1-day--old) lambs, BTP exposure throughout gestation is associated with fewer gonocytes as well as an increased incidence of Sertoli-cell-only (SCO) seminiferous tubules (Elcombe et al., 2021). This study also indicated that there may be two phenotypic responses to EC exposure within male lambs, one in which lambs are more susceptible to disruption and another which appears resistant. This observation mirrors findings in the testes of 19-month-old offspring exposed to BTP *in utero* and for seven months post-natal, where a subset of animals was identified that had reduced germ cell numbers and an increased incidence of SCO seminiferous tubules (Bellingham et al., 2012).

There is currently no information on the effects gestational BTP exposure has on testicular development between parturition and adulthood. Puberty in male sheep begins at approximately 8 weeks of age, therefore the aim of the current study was to examine the morphology and transcriptome of gestationally BTP exposed prepubertal (8-week-old) ram lamb testes to gain insights into the mechanisms underlying observed adverse morphological observations and potential functional outcomes.

2. Methods

2.1. Ethics statement

All animals were maintained under normal husbandry conditions at the University of Glasgow Cochno Farm and Research Centre. The research programme was approved by the University of Glasgow School of Veterinary Medicine Research Ethics Committee. All procedures were conducted in accordance with the Home Office Animal (Scientific Procedures) Act (A(SP)A), 1986 regulations under licence (PPL PF10145DF).

2.2. Experimental animals

EasyCare ewes were maintained on pastures fertilised with either biosolids, at conventional rates (4 tonnes/ha, twice per annum (April/September); biosolids exposed (B)), or with inorganic fertiliser at a rate which supplied equivalent levels of nitrogen (225 kg N/ha per annum; control (C)) for one month prior to mating and for the duration of pregnancy. Mating was by artificial insemination with semen from 4 rams which had only been maintained on control pasture. Ewes were maintained indoors for the final two weeks of pregnancy and fed forage supplemented with concentrates as per normal husbandry practice. Biosolids-exposed ewes received forage harvested from biosolids-treated pastures. After parturition, all ewes and lambs were maintained on control pastures. Therefore, all EC exposure was maternal (i.e., through placental or lactational transfer). At 8-weeks of age, a subset of male offspring from ewes exposed to conventionally fertilised pastures (n = 11 ram lambs from separate mothers and balanced across sires (C)) and biosolids treated pastures (BTP) (n = 11 rams from separate mothers and balanced across sires (B)), were weighed before euthanasia by intravenous barbiturate overdose (140 mg/kg Dolethal, Vetroquinol, UK) for tissue collection.

2.3. Tissue collection

Testes were removed at necropsy. Two transverse slices were taken from the centre of the left testis, fixed overnight in 10% neutral buffered formalin (Thermo Scientific – 16499713), then transferred to 70% ethanol (VWR – 20821.330) prior to processing, and embedding in paraffin wax for histology (Excelsior AS, Thermo Scientific). A 5 mm thick transverse slice was taken from the centre of the right testis and frozen on dry ice prior to storage at − 80 °C until RNA extraction.

2.4. Immuno-histochemistry

Formalin-fixed paraffin embedded testicular tissues were sectioned (5 μm) using a microtome (Leica Biosystems, model RM2125RT). Immuno-histochemistry for DDX4 was used to identify germ cells. Fluorescent immuno-histochemistry was used to localise HIF1α.

For DDX4 immuno-histochemistry, one section per animal was mounted on a Polysine® coated glass slide, dewaxed, and processed for antigen retrieval (autoclave for 21 min while immersed in citrate buffer 10 mM, pH 6). Slides were washed in TBS and taken through peroxidase, avidin, and biotin blocking solutions (15 min each with TBS washes in between). Non-specific binding was blocked by incubation for 30 mins

with 20% goat serum in TBS before incubation with the primary antibody (rabbit anti-DDX4 polyclonal antibodies; Abcam – ab13840) diluted 1:1000 in antibody diluent (Agilent DAKO – S2022) overnight at 4 °C. Sections were then washed in TBS + 1% Tween20 before being incubated for 30 min with a biotinylated secondary antibody (goat anti-rabbit biotinylated polyclonal antibodies; Agilent DAKO – E0432) diluted 1:200 in antibody diluent. Following incubation in secondary antibody, sections were treated with Vectastain ABC-HRP system (Vector Laboratories – PK4000) for 60 min before being washed in TBS + 1% Tween20 and stained using DAB for 30 s. Slides were then washed in TBS, and counter-stained with haematoxylin and coverslips mounted using DPX.

For HIF1α fluorescent immuno-histochemistry, one section per animal was mounted on a Polysine® coated glass slide, dewaxed, and processed for antigen retrieval (microwaved at medium heat in 1 mM EDTA, pH 8.0, for 10 min). Slides were washed in TBS and incubated overnight at 4 °C with mouse anti-HIF1α antibodies (Invitrogen – MA1–16504) diluted 1:250 in 5% BSA / TBS-T. Slides were washed with TBS and incubated for 1 h at room temperature with goat anti-mouse antibodies (Abcam – ab150113) diluted 1:1000 in 5% BSA / TBS-T. Sections were counter stained with DAPI (Abcam – ab104139) and cover-slipped.

2.5. Image capture and analysis

For DDX4 immuno-histochemistry, four images of the lobuli testis were captured (Leica DM4000B microscope with a Leica DC480 digital camera at 100x magnification using Leica Qwin software) from separate areas (top, bottom, left, and right) of each tissue section for each animal, as previously performed (Elcombe et al., 2021). Using ImageJ (version 1.53a), all individual tubules which were entirely captured within images were manually selected (n = 2145 Control, 3673 Biosolid). DDX4 positive and negative cells were counted by automated macro (pre-validated on a subset of data – Supplementary Data 1). Mean germ cell to total cell populations, per tubule, were calculated relative to the mean control, as well as the proportion of seminiferous tubules without germ cells (Sertoli-cell-only; SCO). Separately, tubule selections were filtered for circularity using the equation $4\pi(Area/Perimeter)^2$ with a threshold of ≥ 0.9 (n = 587 Control, 1326 Biosolid) and minimum Feret's diameters measured. Additional images were taken at 400x magnification for increased visual detail but were not part of the analysis.

For HIF1α fluorescent immuno-histochemistry, four representative images of the lobuli testis were captured (Leica DM4000B microscope with a Leica DC480 digital camera at 400x magnification using Leica Qwin software) from separate areas (top, bottom, left, and right). Using ImageJ, all areas out-with seminiferous tubules were manually selected and co-localisation analysis performed using the JACoP plugin (Bolte and Cordelières, 2006), which provided Maders' overlap coefficients for the proportion of HIF1α staining that overlapped DAPI staining.

2.6. RNA extraction, cDNA library preparation, sequencing, and data analysis

Transcriptome analysis was performed as previously described (Elcombe et al., 2021). Briefly, RNA was extracted, purified, reverse transcribed, and ligated to individual DNA barcodes for multiplexing. As the barcoding kit only contains twelve individual barcodes, samples were split into two groupings of eleven (mixed control and biosolids) for sequencing. Barcoded cDNA samples within a grouping were pooled and sequenced using a MinION Nanopore sequencer (Oxford Nanopore). Data were processed and filtered for quality prior to alignment to the reference transcriptome (constructed from NCBI's Oar_v4.0 reference genome and annotation files) and counted. Aligned data was archived to EMBL's European Bioinformatics Institute, ArrayExpress accession number E-MTAB-11645. Batch effects were assessed by BatchQC (Manimaran et al., 2016). Differential gene expression (DGE) analysis was performed on gene counts by EdgeR. Differentially expressed genes (DEGs) were called using a p-value threshold of 0.05, $\log_2$ fold change threshold of < -1 or > 1, and false discovery rate (FDR) threshold of 0.1. Gene ontology (GO) analysis was performed using DEG lists in DAVID (version 6.8).

2.7. Quantitative qPCR

RNA was extracted from approximately 30 mg of frozen testes using RNeasy Mini Kit (Qiagen – 74104). Genomic DNA was degraded and cDNA synthesised using QuantiTect Reverse Transcription Kit (Qiagen – 205311). qPCR was performed using qPCR Brilliant II SYBR Master Mix (Agilent – 600828) on a Stratagene 3000 qPCR system. Primer details can be found in Supplementary Data 2. Raw fluorescent data were regressed by PCR Miner (Zhao and Fernald, 2005) to produce primer efficiencies and Ct values which were used in ΔΔCt analysis to produce Log_2 Fold Change values.

2.8. Western blots

Approximately 15 mg of frozen tissue samples were homogenised using a 1 mL tapered PTFE tissue homogeniser into 19x volume of RIPA buffer (150 mM NaCl, 1% Triton X-100, 0.5% Sodium deoxycholate, 0.1% SDS, 50 mM Tris (pH 8.0)) containing protease inhibitors (Merck – 11697498001) and phosphatase inhibitors (Merck – 4906845001). Samples were centrifuged at 12,000 x *g* for 20 min at 4 °C. Following protein determination (Thermo Scientific – 23227), samples were made to a final concentration of 2 μg/μL using LDS Sample Buffer (Invitrogen – NP0007) and Reducing Agent (Invitrogen – NP0004) and heated to 95 °C for 10 min. 10 μL of reduced, denatured samples (20 μg protein) were loaded into wells of 4–12%, Bis-Tris, 1.0 mm acrylamide gels (Invitrogen – WG1403BOX) using 5 μL of protein reference standard (BioRad – 1610375EDU) in the first and last wells. Gels were run under constant voltage using MOPS SDS Running Buffer (Invitrogen – NP0001) with added antioxidant (Invitrogen – NP0005) and transferred to nitrocellulose membranes (Invitrogen – IB23001 NC) using an iBlot2 (Invitrogen – IB21001). Membranes were blocked using Intercept TBS Blocking Buffer (Licor – 927–60001), washed with TBS-T and TBS, and incubated overnight with primary antibody diluted 1:1000 in 5% BSA/TBS at 4 °C. The next morning membranes were washed with TBS-T and TBS before incubation in secondary antibody diluted 1:10,000 in 5% BSA/TBS at room temperature for one hour. Membranes were then washed in TBS-T, TBS, and finally MilliQ water before imaging on an Odyssey DLx Imager (Licor – 9142). Primary antibodies used were mouse-anti-HIF1α monoclonal (Invitrogen – MA1–16504) and rabbit-anti-α-tubulin polyclonal (Invitrogen – PA1–38814), with donkey anti-mouse (Invitrogen – SA5–10172) and donkey anti-rabbit (Invitrogen – SA5–10044) fluorophore conjugated secondary antibodies. Fluorescent intensities were quantified using Licor Image Studio Software (version 5.2.5). HIF1α signal intensities were normalised to α-Tubulin and expressed as relative to the average of control values.

2.9. BaseSpace analysis

Illumina's BaseSpace correlation Engine enables the comparison and correlation of DEG datasets through a combination of ranked-based enrichment statistics, meta-analyses, and biomedical ontologies (Kupershmidt et al., 2010). BaseSpace correlation Engine employs a rank-based, nonparametric analysis strategy driven by a Running Fisher's test algorithm which performs the rank-based directional enrichment process. This enrichment process utilises a Fisher's exact test to calculate four p-values: two p-values for the genes which are positively correlated between the datasets (genes that are either up or down-regulated in both datasets) and two for the negatively correlated genes (genes that are up-regulated in dataset 1 and down-regulated in dataset 2, or vice versa). The overall correlation p-value was calculated

by converting the four p-values to -$\log_{10}$ p-values and subtracting the sum of the negative correlation p-values from the sum of the positive correlation p-values. A p-value threshold for significance of 0.0001 was used. To enable cross-platform and cross-species comparisons BaseSpace correlation engine software uses a database compiled of commonly used gene identifiers and reference identifiers along with ortholog information to standardise mapping across platforms and species.

Expression data for DEGs with $p \leq 0.05$ were analysed for correlation to published data by Illumina's BaseSpace software. Positively correlating DEGs were filtered for those common across each dataset per study. These gene lists were then combined and submitted to DAVID for pathway and GO analyses.

2.10. Effect of changes to cellularity

To assess the effect of changes in testicular cellular composition, DEGs with pathways or GO terms identified as enriched were tested for correlation using generalised linear models, on gene counts against the geometric mean of gene counts for germ cell specific biomarkers, and p values corrected for false discovery. Germ cell specific biomarkers used were *CD9*, *CD14*, *THY1*, *NOTCH1*, *GFRA1*, *CDH1*, and *UCHL1*.

2.11. Statistical analysis

All calculations and statistical analyses were performed in R (version 4.1.1) using base functionality. Unless otherwise stated, data were fitted to generalised linear models with gamma distribution and groups compared by Wald tests using the glm() and summary() base R functions. Models accounted for genetic structure of the data by incorporating sire heritage into calculations. Plots were created using the R package ggplot2 (version 3.3.5). Data are presented as mean ± SD.

3. Results

3.1. Fewer germ cells and more frequent Sertoli-cell only seminiferous tubules in testes of prepubertal rams prepubertal gestationally exposed to BTP

Histopathology was performed to assess effects of gestational BTP exposure on gross testes morphology and cellularity. Following immunohistochemistry for DDX4, representative images from control (C) and biosolids (B) testes are shown in Fig. 1 at 100x magnification (A and C) and 400x magnification (B and D). The mean relative germ cell: Sertoli cell ratio (Fig. 1E) was lower ($p = 0.014$) in B (0.67 ± 0.22) compared to C lambs (1.00 ± 0.29). The mean percentage of SCO seminiferous tubules (Fig. 1F) was higher ($p = 0.0082$) in B (12.56 ± 11.49%) compared to C lambs (2.27 ± 1.81%). The mean minimum Feret's diameter of seminiferous tubules (Fig. 1E) was smaller ($p = 0.013$) in B (77.51 ± 16.51 μm) than in C (94.89 ± 13.36 μm) lambs.

3.2. Gestational BTP exposure alters testicular transcriptome in prepubertal sheep

Nanopore transcriptome sequencing was performed to identify gene expression affected by gestational BTP exposure. Differential gene expression (DGE) analysis identified 1382 differentially expressed genes (DEGs) between the B and C groups (726 with higher expression and 656 with lower expression in B relative to C). Ninety-nine DEGs had an FDR ≤ 0.1 (60 with higher expression and 39 with lower expression in B relative to C). A *z*-score heatmap of these genes is shown in Fig. 2 (differential expression data presented in Supplementary Data 3). Gene ontology (GO) analysis of the 99 DEGs indicated 6 GO terms as enriched ($p < 0.05$) (Table 1). Two genes, from different GO term groups (*HFM1* and *SIRT4*), had expression levels which correlated ($p < 0.05$) with the geometric mean of germ cell markers (*CD9*, *CD14*, *THY1*, *NOTCH1*, *GFRA1*, *CDH1*, and *UCHL1*).

3.3. Gestational BTP-induced changes in testicular transcriptome of prepubertal sheep positively correlates with testicular transcriptome of human TDS patients

Illumina's BaseSpace Correlation Engine software was used to identify similar data from public data sets. A positive ($p < 0.0001$) correlation was identified between the biosolids exposed DEG data and human TDS patient testes transcriptome data from 7 published DEG datasets across 3 separate studies (Supplementary Data 4). A gene list was created by identifying correlating DEGs in common across each dataset per study, and then combining between studies. This list comprised of 520 genes and was submitted to DAVID for GO and KEGG pathway analyses, which identified 9 KEGG pathways and 25 GO terms as enriched ($p < 0.05$) (Table 2). Five genes, each from different GO term / KEGG pathway groups (*BCLAF1*, *INPP5A*, *MAPKAP1*, *TBC1D15*, and *VPS41*), had expression levels which correlated ($p < 0.05$) with the geometric mean of germ cell markers (*CD9*, *CD14*, *THY1*, *NOTCH1*, *GFRA1*, *CDH1*, and *UCHL1*).

3.4. Gestational BTP exposure increases expression of genes downstream of mTOR activation

As GO and KEGG analysis identified 2 mTOR terms as enriched, qPCR was performed on a range of genes which are downstream products of mTOR activation. Of the fourteen genes quantified by qPCR (*ACACA*, *ACAD11*, *ACLY*, *ACOX1*, *BIRC5*, *CCND1*, *CPT1A*, *FABP4*, *FASN*, *HK1*, *LDHA*, *LPL*, *PDPK1*, *VEGFA*), four, *FASN* ($p = 0.044$), *HK1* ($p = 0.032$), *PDPK* ($p = 0.033$), and *VEGFA* ($p = 0.036$), were expressed at a significantly higher level in B than in C animals (Fig. 3). Three of these genes (*VEGFA*, *HK1*, and *PDPK1*) are transcribed via Hypoxia Inducible Factor 1 Alpha (HIF1α) activation.

3.5. Gestational BTP exposure increases nuclear localisation of HIF1α in Leydig cells of prepubertal rams

As qPCR results were indicative of HIF1α activation, immunofluorescent-histochemistry and Western blots were performed. Representative images from C and B testes showing immunofluorescent staining for the transcription factor HIF1α and the nuclear marker DAPI are presented in Fig. 4A, with the quantified overlap of HIF1α and DAPI signal (Manders' overlap coefficient) presented in Fig. 4B. In Leydig cells, a greater ($p = 0.0032$) proportion of HIF1α was seen in the nucleus of B (0.40 ± 0.11) compared to C (0.25 ± 0.10) animals.

Western blots for HIF1α and α-Tubulin are shown in Fig. 4C with the mean relative normalised abundance of HIF1α in the testes of C and B animals shown in Fig. 4D. There was less ($p = 0.0077$) HIF1α detected in the testes of B (0.71 ± 0.22) than C (1.00 ± 0.29) animals.

4. Discussion

The present study demonstrates the ability for gestational exposure to complex, low-level, real-life chemical mixtures to adversely affect prepubertal testis development. Similarities between morphological and gene expression patterns seen in biosolids exposed lambs and human TDS patients suggest that the changes observed prior to puberty in this model may predispose animals to a TDS-like phenotype and demonstrates the model's utility to investigate the pathogenesis of TDS. Of specific note, biosolids exposure was associated with differential expression of genes related to apoptotic processes and mTOR signalling, and increased expression of a group of mTOR regulated genes which are all transcriptionally controlled by a common nuclear factor (i.e., HIF1α). The expression and activation of HIF1α was also found to be altered. Specifically, HIF1α protein levels were lower in B lamb testes and expression was more localised to the nuclei of Leydig cells. As HIF1α is known to inhibit STAR transcription and testosterone synthesis (Wang et al., 2019), and gestational BTP exposure has been associated with

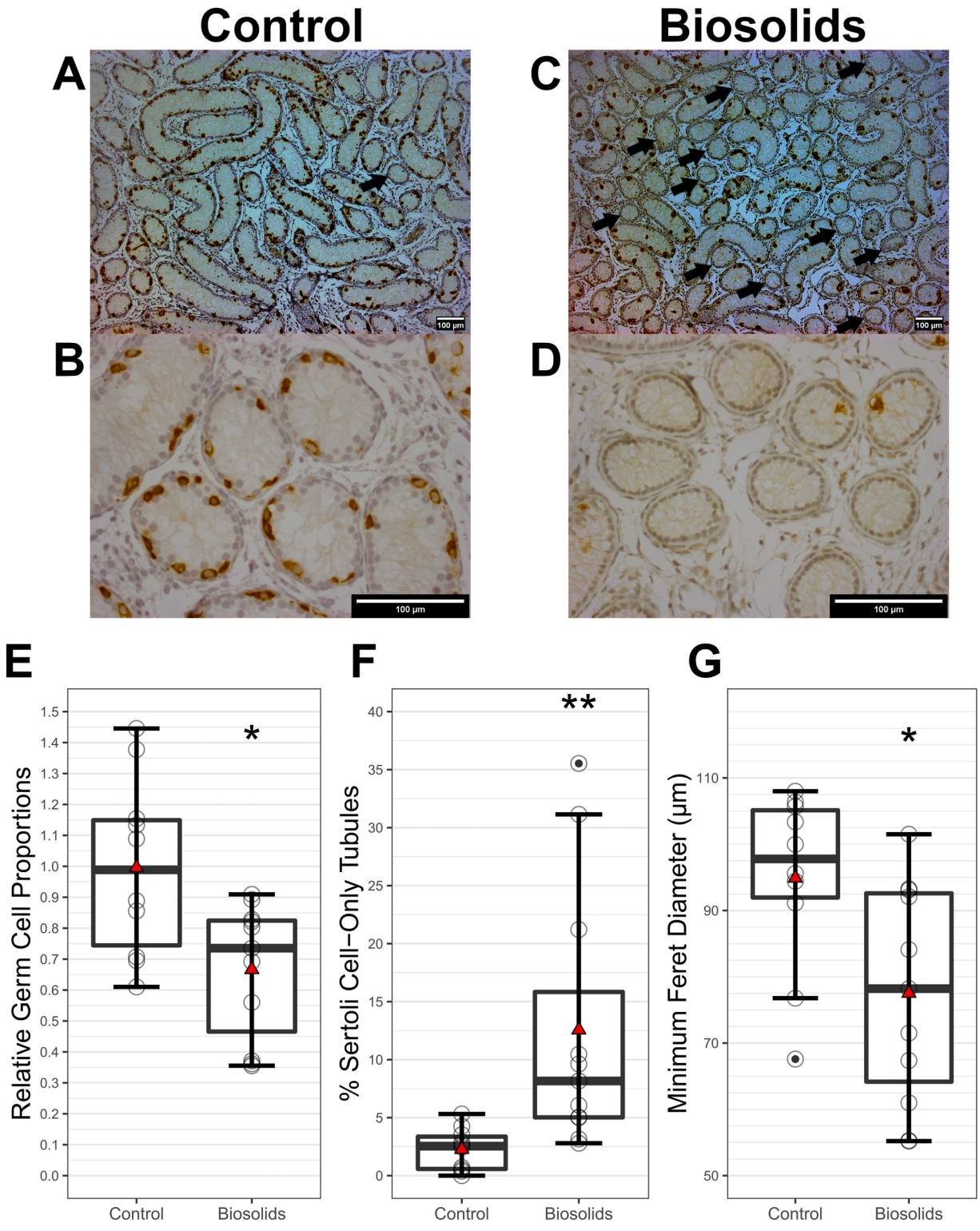

Fig. 1. Histopathological findings in 8-week-old control and biosolids-exposed lamb testes (n = 11 per group). Representative images of haematoxylin / DDX4-DAB stained tissue sections from 8-week-old control and biosolids lambs, taken with a magnification of 100x (A and C respectively) and 400x (B and D respectively). Scale bars (bottom right of images) show 100 µm. Arrows indicate Sertoli-cell-only (SCO) seminiferous tubules. Relative proportions of germ cells to Sertoli cells (E) and percent of tubules which were SCO (F) ($p = 0.014$ and $p = 0.0082$ respectively). Seminiferous tubule minimum Feret's diameters ($p = 0.013$) (G). Boxes represent 25th to 75th percentile, horizontal bar indicates 50th percentile, whiskers indicate range excluding outliers, solid filled circles show outliers, open circles show individual data points, and red triangles show means.

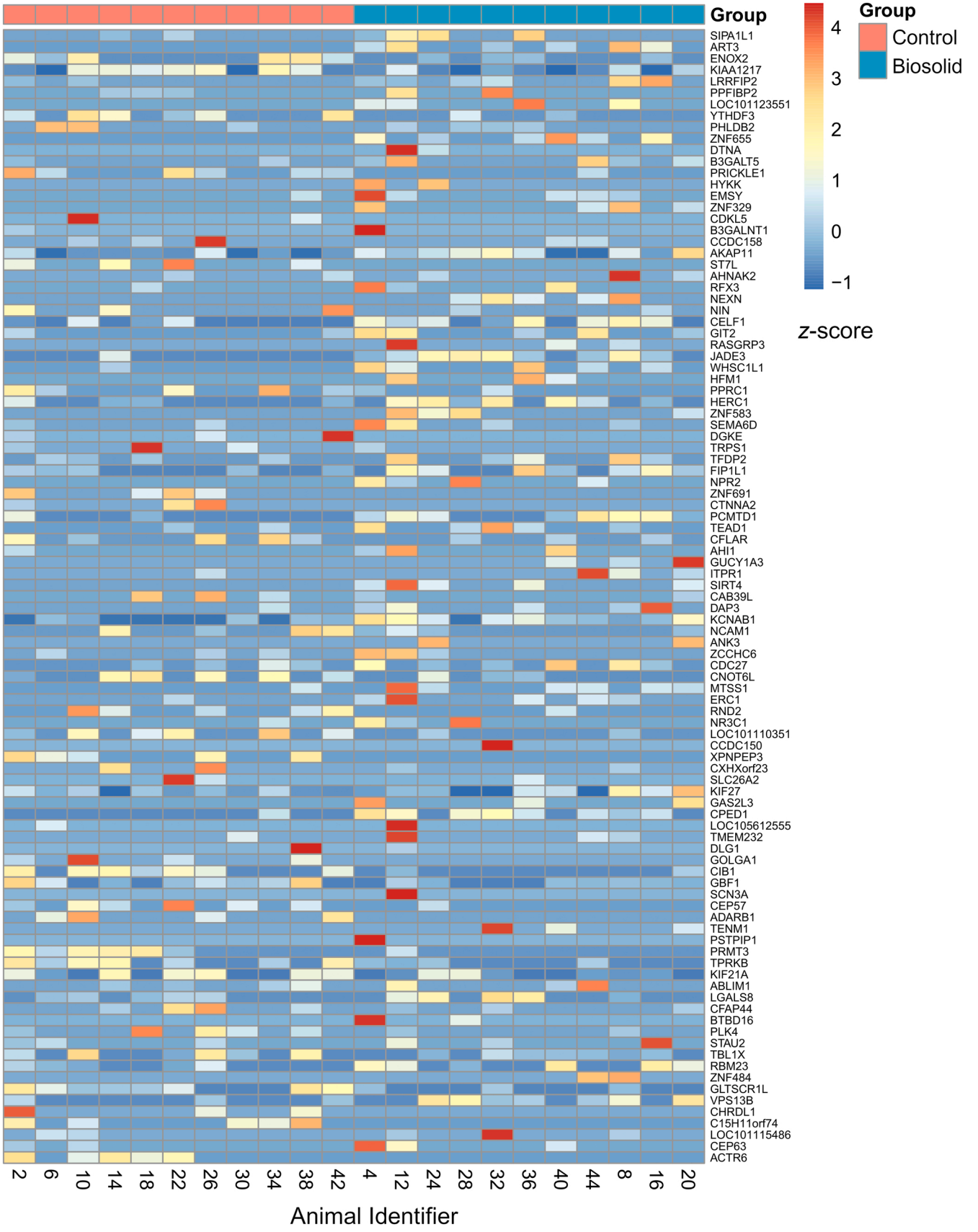

Fig. 2. Heat map of DEGs plotted against z-score. Genes are ordered from top to bottom by increasing p-value.

Table 1
GO terms identified as enriched in the list of 99 DEGs with FDR < 0.1 by DAVID.

Category	GO Term	Fold Enrichment	*p*-value
Cellular Component	Centrosome	4.03	0.0156
Molecular Function	Nucleic acid binding	2.96	0.0160
Biological Process	Spermatid development	9.60	0.0379
Cellular Component	Node of Ranvier	47.01	0.0412
Molecular Function	Guanylate cyclase activity	45.21	0.0427
Biological Process	Regulation of transcription, DNA-templated	2.95	0.0498

lower serum testosterone levels in fetal and neo-natal offspring (Elcombe et al., 2021; Lea et al., 2022), these changes in HIF1α may provide mechanistic reasoning to the testicular phenotype of biosolids exposed males.

There is increasing evidence of synergistic actions between different chemical components within low dose chemical mixtures leading to adverse effects on male gonadal development. In rodent studies, male offspring exposed gestationally to low doses of some simple chemical mixtures (≤ 10 components) exhibit under-masculinised (aka feminised) phenotypes, genital malformations, pathological testicular morphology, and impaired spermatogenesis (Buñay et al., 2018; Christiansen et al., 2009; Hass et al., 2012; Jacobsen et al., 2012; Rider et al., 2008). The present study found that following gestational exposure to a complex chemical mixture (similar to human exposure) prepubertal male offspring exhibit fewer testicular germ cells and more frequent Sertoli-cell-only seminiferous tubules; a phenotype resemblant of morphological differences in the testes of the late gestation fetus (Paul et al., 2005), neonatal lamb (Elcombe et al., 2021), and a subset of adult offspring (Bellingham et al., 2012) following similar exposure. Importantly, this testicular phenotype also resembles mixed testicular atrophy, a hallmark of TDS in humans (Nistal et al., 2017; Skakkebæk et al., 2001). Despite the repeatable histological changes seen in the BTP sheep testes, other anatomical correlates of the TDS phenotype of humans (i.e., cryptorchidism, hypospadias, etc) have not been described specifically in BTP exposed sheep. This is likely due to the limited number of animals studied. While these developmental abnormalities are rare in sheep, around 0.1–0.7% cryptorchidism and 0.9% hypospadias (Amann and Veeramachaneni, 2007; Smith et al., 2012b), which may reflect regional incidences in rams selected for culling (Smith et al., 2012a), it is of note that a sibling of one biosolid sheep included in this study was cryptorchidic.

DGE analysis of the testicular transcriptome was undertaken to identify the mechanism by which exposure to the complex mixture of ECs present within biosolids leads to pathogenic changes in testicular morphology. This analysis indicated decreased testicular expression of genes involved in maintaining the blood-testes barrier (BTB) and cell polarity (*PRICKLE, CTNNA2,* and *DLG1*) (Paul and Robaire, 2013; Su et al., 2012; Wang et al., 2022). BTB and cell polarity maintenance are crucial for spermatogonial stem-cell survival, differentiation, and spermatid development (Chen and Cheng, 2016; Mruk and Cheng, 2015). Also poorly expressed in B animals was the gene *ADRB1* (*ADAD2* in humans), which is crucial for male germ cell differentiation, and potentially causative in cohorts of human patients with spermatogenic maturation arrest (Krausz et al., 2020; Snyder et al., 2020). EC exposure also reduced expression of genes essential for spermatogenesis (*CIB1, GBF1, CFAP44,* and *PLK4*) (Au et al., 2015; Miyamoto et al., 2016; Tang et al., 2017; Yuan et al., 2006). EC effects on spermatogenesis were also highlighted by significant enrichment of the GO term "Spermatid Development". All identified DEGs were tested for correlations to the geometric mean of known germ cell markers to assess the impact of changes to testicular cellularity. However, as only around 2% of genes showed a significant correlation, any effect was deemed minimal. Comparison of the DEG data from this study with DEG data from independent studies in human TDS patients revealed complementarity between the sheep model and TDS patient data and identified EC-responsive genes which may lead to testicular dysfunction. Correlating DEGs between biosolids-exposed animals and TDS patients were also tested against the geometric mean of known germ cell markers. As

Table 2
GO terms and KEGG pathways identified as potentially enriched by DAVID within the list of common DEGs between the biosolids data and at least one correlating study identified by BaseSpace.

Category	Term	Fold Enrichment	*p*-value
GO: Cellular Component	Cytosol	2.00	0.000030
GO: Molecular Function	Zinc ion binding	1.75	0.000140
GO: Cellular Component	Nucleolus	2.04	0.000285
GO: Cellular Component	Intracellular ribonucleoprotein complex	6.03	0.000926
GO: Molecular Function	mRNA 3'-UTR binding	7.51	0.000999
KEGG	Cell cycle	3.52	0.001055
GO: Cellular Component	Early endosome	3.16	0.002503
GO: Molecular Function	Hydrolase activity	3.98	0.003734
KEGG	Purine metabolism	2.76	0.004030
GO: Biological Process	Apoptotic process	3.88	0.004223
KEGG	Metabolic pathways	1.45	0.007357
GO: Biological Process	mTOR signalling	8.96	0.008819
KEGG	Lysine degradation	4.51	0.010057
GO: Molecular Function	GTPase activator activity	2.61	0.014330
KEGG	ErbB signalling pathway	3.33	0.018098
GO: Biological Process	Ras protein signal transduction	4.70	0.020505
GO: Molecular Function	DNA-directed DNA polymerase activity	6.59	0.021242
GO: Biological Process	Positive regulation of gene silencing by miRNA	12.48	0.021909
GO: Cellular Component	mTORC2 complex	11.95	0.024152
GO: Molecular Function	DNA-dependent ATPase activity	5.96	0.027828
GO: Biological Process	Mitochondrial fragmentation involved in apoptotic process	10.92	0.028559
GO: Biological Process	Protein localization to microtubule	10.92	0.028559
KEGG	Pyrimidine metabolism	2.98	0.029146
GO: Biological Process	Platelet-derived growth factor receptor signalling pathway	5.82	0.029464
GO: Molecular Function	RNA polymerase II core promoter proximal region sequence-specific DNA binding	1.92	0.030620
GO: Cellular Component	Nucleus	1.25	0.032457
GO: Biological Process	Retrograde transport, endosome to Golgi	4.04	0.033621
KEGG	Phosphatidylinositol signalling system	2.86	0.034587
GO: Biological Process	Peptidyl-tyrosine autophosphorylation	9.71	0.035899
GO: Molecular Function	ATP binding	1.32	0.036382
KEGG	Biosynthesis of antibiotics	2.07	0.039467
GO: Biological Process	Negative regulation of viral transcription	8.74	0.043875
KEGG	Base excision repair	5.01	0.044115
GO: Biological Process	Mitochondrion organization	4.85	0.047341

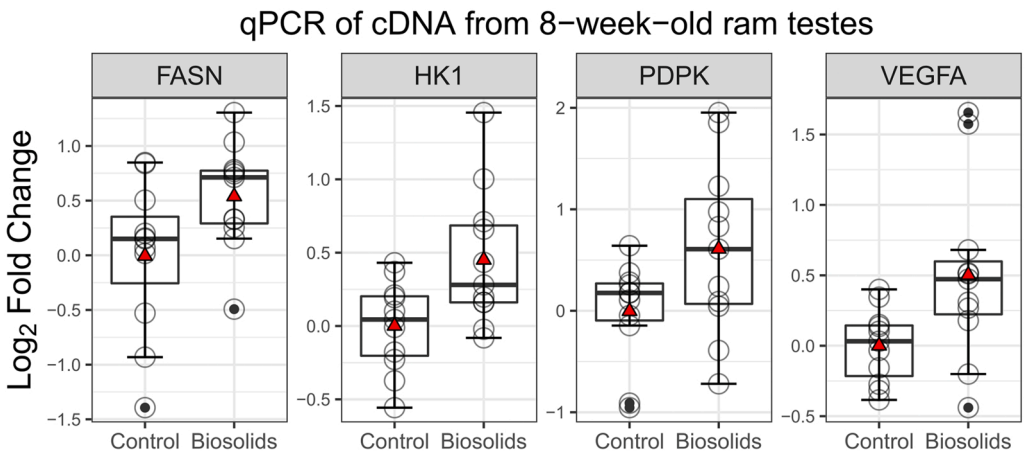

Gene	p value	Sig
FASN	0.04355	*
HK1	0.03201	*
PDPK	0.03337	*
VEGFA	0.03550	*

Fig. 3. Log_2 fold change of testicular gene expression between biosolids-exposed and control animals (n = 11 per group). Boxes represent 25th to 75th percentile, horizontal bar indicates 50th percentile, whiskers indicate range excluding outliers, solid filled circles show outliers, open circles show individual data points, and red triangles show means.

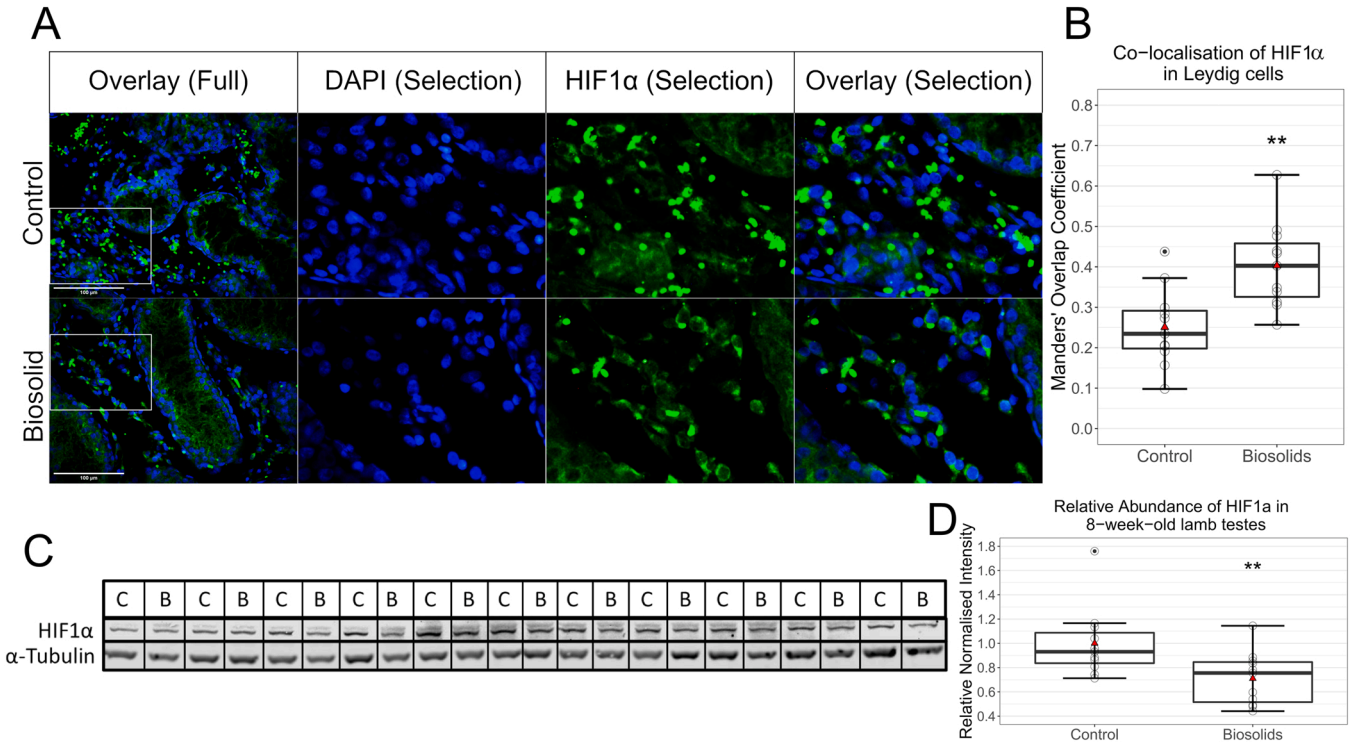

Fig. 4. HIF1α in testes (n = 11 per group). Immunofluorescent staining of testes sections (A). Images to the right are of selections seen in images to the left, which were taken at 400x magnification. Blue staining is of DAPI and green of HIF1α. Scale bars (bottom left in overlay images) show 100 μm. Co-localisation analysis (B) performed on regions outside of seminiferous tubules shows significantly (p = 0.0032) more nuclear localisation of HIF1α in Leydig cells of biosolids-exposed animals than control. Manders' Overlap Coefficients of the proportion of green signal overlapping with blue signal were determined by ImageJ. Western blots for HIF1α and α-Tubulin (C and D) show less (p = 0.0077) HIF1α in testes of biosolids-exposed animals than controls. Boxes represent 25th to 75th percentile, horizontal bar indicates 50th percentile, whiskers indicate range excluding outliers, solid filled circles show outliers, open circles show individual data points, and red triangles show means.

< 1% of genes showed a significant correlation, any effect from changes to testicular cellularity was also deemed minimal. Of the GO terms and KEGG pathways identified from correlating DEGs between sheep and TDS patient data, two were mTOR and two were apoptotic entries. mTOR is a crucial component of proper testicular development and spermatogenesis (Correia et al., 2020) and mTOR-related pathways have previously been identified in the BTP sheep testicular transcriptome at GD140 (Lea et al., 2022) and in 1-day-old neonates (Elcombe et al., 2021). This would suggest it is a developmentally stable alteration.

Given the recognised role of mTOR in testicular development, to investigate the effects of biosolids exposure further the expression of a selection of genes which are upregulated following mTOR activation (Laplante and Sabatini, 2013) was investigated. Of the fourteen genes examined, the testicular expression of four genes was increased in B lambs. Of these, three (*VEGFA, HK1*, and *PDPK1*) are involved in the angiogenic and metabolic adaptive responses to hypoxia via Hypoxia Inducible Factor 1 Alpha (HIF1α) activation (Child et al., 2021), indicating a potential common point of EC action.

HIF1α is an important factor in embryonic development which is expressed from early embryonic stages, continuing in germ cells and other tissues into adulthood (Takahashi et al., 2016). Under normoxic conditions, HIF1α is tightly controlled and swiftly degraded via polyubiquitination-mediated proteolysis (Child et al., 2021). Under hypoxic conditions, however, the mechanisms for degradation are suppressed and nuclear translocation of HIF1α occurs, which ultimately increases the expression of genes largely involved in angiogenic and metabolic reprogramming (Child et al., 2021). HIF1α activation can also occur independently of oxygen status, triggered by biochemical pathways such as mTOR (Dodd et al., 2015) or small molecules and reactive oxygen species (Bonello et al., 2007; Xia et al., 2009). HIF1α activation in the testes of B animals is likely an adaptive response, as VEGFA and PDPK1 are both critical for spermatogonial stem-cell survival (Fu et al., 2018; Sargent et al., 2016). However, HIF1α activation may have also factored in the observed adverse outcome. HIF1α expression within the testes is highest in Leydig cells (Palladino et al., 2011), a primary function of which is testosterone production. HIF1α has been shown to repress STAR transcription in Leydig cells by way of binding site blocking (Wang et al., 2019). As STAR is the main rate-limiting step in steroid biosynthesis (Manna et al., 2016) a decrease in STAR would be expected to reduce testosterone synthesis, which has also been observed in Leydig cells following HIF1α activation (Wang et al., 2019). While total testicular HIF1α content was reduced in B lambs, there was also a greater proportion of HIF1α localised within the nuclei of the Leydig cells of B animals. However, changes in HIF1α protein levels may be attributable to changes in cellularity and loss of germ cell HIF1α. Additionally, the magnitude of change in HIF1α nuclear localisation (160% of control) outweighs the magnitude of change in HIF1α protein levels (71% of control). Therefore, despite lower overall HIF1α protein levels in the whole testes, it is evident that this was overcome and overall BTP exposure resulted in more activated HIF1α within the nucleus of Leydig cells. An overall EC induced increase in nuclear-localised HIF1α in Leydig cells, as seen in the B animals in the current study, could explain the lower testosterone levels reported in fetal and neonatal B lambs (Elcombe et al., 2021; Lea et al., 2022).

While the present study demonstrates the ability for a complex, low-level, real-life chemical mixture to elicit an adverse effect on the testes of gestationally exposed animals, there are limitations. A major limitation is the lack of knowledge on the precise oral dosage. While the chemical mixture complexity provided by biosolids is a strength of the model in terms of relevance to humans, it also presents a challenge with respect to dose determination. There are published quantifications of various chemicals in organs of directly and gestationally exposed animals (Bellingham et al., 2012; Filis et al., 2019; Rhind et al., 2010, 2009, 2005), but only dioctyl phthalate, octyl phenol, and nonyl phenol have had oral dosage estimations, which were below TDI values (Rhind et al., 2002). There have also been quantifications of 10–12 perfluoroalkyl substances (PFAS) in lettuce, radishes, celery, peas, and tomatoes grown in biosolids fertilised soil, with PFBA and PFPeA having the highest concentrations at $>$ 230 ng/g (Blaine et al., 2014, 2013). It is of note that phthalates, alkylphenols, and PFAS can produce reproductive developmental toxicity in offspring when administered individually at higher doses during gestation (Di Nisio et al., 2019; NAS, 2017; Uguz et al., 2009). However, without precise understanding of dosage, effects from BTP exposure cannot be assessed against mixture toxicity models, and no insight can be gained on possible interactions and/or synergies that may occur. However, this point is somewhat moot as chemical levels are generally very low and do not differ significantly from control levels; such is the ubiquity of ECs, most are also detectable in control pastures (Evans et al., 2014; Rhind et al., 2010, 2002, 2013). There is also considerable inter-animal variation in organ chemical load (Bellingham et al., 2012; Filis et al., 2019; Rhind et al., 2010, 2009, 2005) resulting from biosolids batch variance, grazing area preferences, and differential uptake across treated pastures. Another significant limitation of the model is the practicalities and resources required to undergo such investigations. Unlike traditional rodent studies, sheep require a great deal of resources, both physical and human. As such, animal numbers and time points are limited. This compounds with the outbred nature of sheep, which is again an advantage in terms of relevance to humans but a disadvantage in terms of complexity. Consequentially, diametric responses to gestational BTP exposure are to be expected, as have indeed been seen previously (Bellingham et al., 2012; Elcombe et al., 2021). This can complicate result interpretation and can be reasonably assumed to mask more subtle effects.

Fetal development is a complex and dynamic period during which there is increased vulnerability to xenobiotic induced toxicity. This study demonstrates that *in utero* exposure to a complex mixture of chemicals that reflects real-life human exposure results in anatomical and molecular changes in the prepubertal testes. It is the first study to show commonality between transcriptomic profiles of a low-level EC exposure animal model and human TDS patients. Investigation of the DEGs common to the model and TDS patients led to evidence of exposure-induced changes to HIF1α activation in Leydig cells, which is linked to steroid biosynthesis. These findings add to the body of evidence to suggest that exposure to real-world levels of environmental chemical mixtures during pregnancy may have an adverse effect on male offspring reproductive health, contributing to the decline in human sperm quality and fecundity.

Funding

This work was funded by the National Institute of Environmental Health Sciences, USA, grant R01 ES030374.

CRediT authorship contribution statement

Chris S. Elcombe: Conceptualization, Methodology, Formal analysis, Investigation, Data curation, Writing – original draft. **Ana Monteiro:** Methodology, Investigation. **Matthew R. Elcombe:** Methodology, Investigation. **Kevin D. Sinclair:** Writing – review & editing. **Richard Lea:** Writing – review & editing, Vasantha Padmanabhan, Writing – review & editing. **Mohammad Ghasemzadeh-Hasankolaei:** Writing – review & editing. **Neil P. Evans:** Conceptualization, Methodology, Writing – review & editing, Supervision. **Michelle Bellingham:** Conceptualization, Methodology, Writing – review & editing, Supervision.

Declaration of Competing Interest

The authors have no conflicts of interest to declare and have not participated in, nor anticipate participation in, any legal, regulatory, or advocacy proceedings related to the contents of the paper. The authors declare that they have no known competing financial interests or personal relationships that could have appeared to influence the work reported in this paper.

Acknowledgments

We are grateful to the staff at Cochno Farm and Research Centre for their technical assistance.

Appendix A. Supporting information

Supplementary data associated with this article can be found in the online version at doi:10.1016/j.etap.2022.103913.

References

Amann, R.P., Veeramachaneni, D.N.R., 2007. Cryptorchidism in common eutherian mammals. Reproduction 133, 541–561. https://doi.org/10.1530/REP-06-0272.
Au, C.E., Hermo, L., Byrne, E., Smirle, J., Fazel, A., Simon, P.H.G., Kearney, R.E., Cameron, P.H., Smith, C.E., Vali, H., Fernandez-Rodriguez, J., Ma, K., Nilsson, T.,

Bergeron, J.J.M., 2015. Expression, sorting, and segregation of Golgi proteins during germ cell differentiation in the testis. Mol. Biol. Cell 26, 4015–4032. https://doi.org/10.1091/mbc.E14-12-1632.

Bellingham, M., Fowler, P.A., Amezaga, M.R., Rhind, S.M., Cotinot, C., Mandon-Pepin, B., Sharpe, R.M., Evans, N.P., 2009. Exposure to a complex cocktail of environmental endocrine-disrupting compounds disturbs the kisspeptin/GPR54 system in ovine hypothalamus and pituitary gland. Environ. Health Perspect. 117, 1556–1562. https://doi.org/10.1289/ehp.0900699.

Bellingham, M., Mckinnell, C., Fowler, P.A., Amezaga, M.R., Zhang, Z., Rhind, S.M., Cotinot, C., Mandon-Pepin, B., Evans, N.P., Sharpe, R.M., 2012. Foetal and post-natal exposure of sheep to sewage sludge chemicals disrupts sperm production in adulthood in a subset of animals. Int. J. Androl. 35, 317–329. https://doi.org/10.1111/j.1365-2605.2011.01234.x.

Bellingham, M., Amezaga, M.R., Mandon-Pepin, B., Speers, C.J.B., Kyle, C.E., Evans, N. P., Sharpe, R.M., Cotinot, C., Rhind, S.M., Fowler, P.A., 2013. Exposure to chemical cocktails before or after conception - The effect of timing on ovarian development. Mol. Cell. Endocrinol. 376, 156–172. https://doi.org/10.1016/j.mce.2013.06.016.

Bellingham, M., Fowler, P.A., MacDonald, E.S., Mandon-Pepin, B., Cotinot, C., Rhind, S., Sharpe, R.M., Evans, N.P., Mandon-Pepin, B., Cotinot, C., Rhind, S., Sharpe, R.M., Evans, N.P., 2016. Timing of maternal exposure and foetal sex determine the effects of low-level chemical mixture exposure on the foetal neuroendocrine system in sheep. J. Neuroendocrinol. 12444. https://doi.org/10.1111/jne.12444.

Blaine, A.C., Rich, C.D., Hundal, L.S., Lau, C., Mills, M.A., Harris, K.M., Higgins, C.P., 2013. Uptake of perfluoroalkyl acids into edible crops via land applied biosolids: Field and greenhouse studies. Environ. Sci. Technol. 47, 14062–14069. https://doi.org/10.1021/es403094q.

Blaine, A.C., Rich, C.D., Sedlacko, E.M., Hundal, L.S., Kumar, K., Lau, C., Mills, M.A., Harris, K.M., Higgins, C.P., 2014. Perfluoroalkyl acid distribution in various plant compartments of edible crops grown in biosolids-amended soils. Environ. Sci. Technol. 48, 7858–7865. https://doi.org/10.1021/es500016s.

Bolte, S., Cordelières, F.P., 2006. A guided tour into subcellular colocalization analysis in light microscopy. J. Microsc. 224, 213–232. https://doi.org/10.1111/j.1365-2818.2006.01706.x.

Bonello, S., Zähringer, C., BelAiba, R.S., Djordjevic, T., Hess, J., Michiels, C., Kietzmann, T., Görlach, A., 2007. Reactive oxygen species activate the HIF-1α promoter via a functional NFκB site. Arterioscler. Thromb. Vasc. Biol. 27, 755–761. https://doi.org/10.1161/01.ATV.0000258979.92828.bc.

Borch, J., Axelstad, M., Vinggaard, A.M., Dalgaard, M., 2006. Diisobutyl phthalate has comparable anti-androgenic effects to di-n-butyl phthalate in fetal rat testis. Toxicol. Lett. 163, 183–190. https://doi.org/10.1016/j.toxlet.2005.10.020.

Buñay, J., Larriba, E., Patiño-Garcia, D., Cruz-Fernandes, L., Castañeda-Zegarra, S., Rodriguez-Fernandez, M., del Mazo, J., Moreno, R.D., 2018. Differential effects of exposure to single versus a mixture of endocrine-disrupting chemicals on steroidogenesis pathway in mouse testes. Toxicol. Sci. 161, 76–86. https://doi.org/10.1093/toxsci/kfx200.

Carlsen, E., Giwercman, A., Keiding, N., Skakkebaek, N.E., 1993. Evidence for decreasing quality of semen during past 50 years. Obstet. Gynecol. Surv. 48, 200–202. https://doi.org/10.1097/00006254-199303000-00023.

Chen, H., Cheng, C.Y., 2016. Planar cell polarity (PCP) proteins and spermatogenesis. Semin. Cell Dev. Biol. 59, 99–109. https://doi.org/10.1016/j.semcdb.2016.04.010.

Child, F., Frost, J., Shakir, D., Wilson, J.W., Rocha, S., 2021. Transcription | Regulation of gene transcription by hypoxia-inducible factor 1α. In: Encyclopedia of Biological Chemistry III. Elsevier, pp. 480–489. https://doi.org/10.1016/B978-0-12-819460-7.00033-5.

Christiansen, S., Scholze, M., Dalgaard, M., Vinggaard, A.M., Axelstad, M., Kortenkamp, A., Hass, U., 2009. Synergistic disruption of external male sex organ development by a mixture of four antiandrogens. Environ. Health Perspect. 117, 1839–1846. https://doi.org/10.1289/ehp.0900689.

Correia, B., Sousa, M.I., Ramalho-Santos, J., 2020. The mTOR pathway in reproduction: from gonadal function to developmental coordination. Reproduction 159, R173–R188. https://doi.org/10.1530/REP-19-0057.

Crean, A.J., Senior, A.M., 2019. High-fat diets reduce male reproductive success in animal models: a systematic review and meta-analysis. Obes. Rev. 20, 921–933. https://doi.org/10.1111/obr.12827.

Di Nisio, A., Sabovic, I., Valente, U., Tescari, S., Rocca, M.S., Guidolin, D., Dall'Acqua, S., Acquasaliente, L., Pozzi, N., Plebani, M., Garolla, A., Foresta, C., 2019. Endocrine disruption of androgenic activity by perfluoroalkyl substances: clinical and experimental evidence. J. Clin. Endocrinol. Metab. 104, 1259–1271. https://doi.org/10.1210/jc.2018-01855.

Dodd, K.M., Yang, J., Shen, M.H., Sampson, J.R., Tee, A.R., 2015. mTORC1 drives HIF-1α and VEGF-A signalling via multiple mechanisms involving 4E-BP1, S6K1 and STAT3. Oncogene 34, 2239–2250. https://doi.org/10.1038/onc.2014.164.

Elcombe, C.S., Monteiro, A., Ghasemzadeh-Hasankolaei, M., Evans, N.P., Bellingham, M., 2021. Morphological and transcriptomic alterations in neonatal lamb testes following developmental exposure to low-level environmental chemical mixture. Environ. Toxicol. Pharmacol. 86, 103670 https://doi.org/10.1016/j.etap.2021.103670.

Erhard, H.W., Rhind, S.M., 2004. Prenatal and postnatal exposure to environmental pollutants in sewage sludge alters emotional reactivity and exploratory behaviour in sheep. Sci. Total Environ. 332, 101–108. https://doi.org/10.1016/j.scitotenv.2004.04.012.

Evans, N.P., Bellingham, M., Sharpe, R.M., Cotinot, C., Rhind, S.M., Kyle, C., Erhard, H., Hombach-Klonisch, S., Lind, P.M., Fowler, P.A., 2014. Reproduction Symposium: Does grazing on biosolids-treated pasture pose a Pathophysiological risk associated with increased exposure to endocrine disrupting compounds? J. Anim. Sci. 92, 3185–3198. https://doi.org/10.2527/jas.2014-7763.

Filis, P., Walker, N., Robertson, L., Eaton-Turner, E., Ramona, L., Bellingham, M., Amezaga, M.R., Zhang, Z., Mandon-Pepin, B., Evans, N.P., Sharpe, R.M., Cotinot, C., Rees, W.D., O'Shaughnessy, P., Fowler, P.A., 2019. Long-term exposure to chemicals in sewage sludge fertilizer alters liver lipid content in females and cancer marker expression in males. Environ. Int. 124, 98–108. https://doi.org/10.1016/j.envint.2019.01.003.

Fowler, P.A., Dorà, N.J., McFerran, H., Amezaga, M.R., Miller, D.W., Lea, R.G., Cash, P., McNeilly, A.S., Evans, N.P., Cotinot, C., Sharpe, R.M., Rhind, S.M., Dora, N.J., McFerran, H., Amezaga, M.R., Miller, D.W., Lea, R.G., Cash, P., McNeilly, A.S., Evans, N.P., Cotinot, C., Sharpe, R.M., Rhind, S.M., Dorà, N.J., McFerran, H., Amezaga, M.R., Miller, D.W., Lea, R.G., Cash, P., McNeilly, A.S., Evans, N.P., Cotinot, C., Sharpe, R.M., Rhind, S.M., 2008. In utero exposure to low doses of environmental pollutants disrupts fetal ovarian development in sheep. Mol. Hum. Reprod. 14, 269–280. https://doi.org/10.1093/molehr/gan020.

Fu, H., Zhang, W., Yuan, Q., Niu, M., Zhou, F., Qiu, Q., Mao, G., Wang, H., Wen, L., Sun, M., Li, Z., He, Z., 2018. PAK1 promotes the proliferation and inhibits apoptosis of human spermatogonial stem cells via PDK1/KDR/ZNF367 and ERK1/2 and AKT Pathways. Mol. Ther. Nucleic Acids 12, 769–786. https://doi.org/10.1016/j.omtn.2018.06.006.

Hass, U., Boberg, J., Christiansen, S., Jacobsen, P.R., Vinggaard, A.M., Taxvig, C., Poulsen, M.E., Herrmann, S.S., Jensen, B.H., Petersen, A., Clemmensen, L.H., Axelstad, M., 2012. Adverse effects on sexual development in rat offspring after low dose exposure to a mixture of endocrine disrupting pesticides. Reprod. Toxicol. 34, 261–274. https://doi.org/10.1016/j.reprotox.2012.05.090.

Hombach-Klonisch, S., Danescu, A., Begum, F., Amezaga, M.R., Rhind, S.M., Sharpe, R. M., Evans, N.P., Bellingham, M., Cotinot, C., Mandon-Pepin, B., Fowler, P.A., Klonisch, T., 2013. Peri-conceptional changes in maternal exposure to sewage sludge chemicals disturbs fetal thyroid gland development in sheep. Mol. Cell. Endocrinol. 367, 98–108. https://doi.org/10.1016/j.mce.2012.12.022.

Hu, G.X., Lian, Q.Q., Ge, R.S., Hardy, D.O., Li, X.K., 2009. Phthalate-induced testicular dysgenesis syndrome: leydig cell influence. Trends Endocrinol. Metab. 20, 139–145. https://doi.org/10.1016/j.tem.2008.12.001.

Ilacqua, A., Izzo, G., Emerenziani, G., Pietro, Baldari, C., Aversa, A., 2018. Lifestyle and fertility: the influence of stress and quality of life on male fertility. Reprod. Biol. Endocrinol. 16, 115. https://doi.org/10.1186/s12958-018-0436-9.

Jacobsen, P.R., Axelstad, M., Boberg, J., Isling, L.K., Christiansen, S., Mandrup, K.R., Berthelsen, L.O., Vinggaard, A.M., Hass, U., 2012. Persistent developmental toxicity in rat offspring after low dose exposure to a mixture of endocrine disrupting pesticides. Reprod. Toxicol. 34, 237–250. https://doi.org/10.1016/j.reprotox.2012.05.099.

Kortenkamp, A., 2014. Low dose mixture effects of endocrine disrupters and their implications for regulatory thresholds in chemical risk assessment. Curr. Opin. Pharmacol. 19, 105–111. https://doi.org/10.1016/j.coph.2014.08.006.

Krausz, C., Riera-Escamilla, A., Moreno-Mendoza, D., Holleman, K., Cioppi, F., Algaba, F., Pybus, M., Friedrich, C., Wyrwoll, M.J., Casamonti, E., Pietroforte, S., Nagirnaja, L., Lopes, A.M., Kliesch, S., Pilatz, A., Carrell, D.T., Conrad, D.F., Ars, E., Ruiz-Castañé, E., Aston, K.I., Baarends, W.M., Tüttelmann, F., 2020. Genetic dissection of spermatogenic arrest through exome analysis: clinical implications for the management of azoospermic men. Genet. Med. 22, 1956–1966. https://doi.org/10.1038/s41436-020-0907-1.

Kupershmidt, I., Su, Q.J., Grewal, A., Sundaresh, S., Halperin, I., Flynn, J., Shekar, M., Wang, H., Park, J., Cui, W., Wall, G.D., Wisotzkey, R., Alag, S., Akhtari, S., Ronaghi, M., 2010. Ontology-based meta-analysis of global collections of high-throughput public data. PLoS One 5. https://doi.org/10.1371/journal.pone.0013066.

Laplante, M., Sabatini, D.M., 2013. Regulation of mTORC1 and its impact on gene expression at a glance. J. Cell Sci. 126, 1713–1719. https://doi.org/10.1242/jcs.125773.

Lea, R.G., Amezaga, M.R., Loup, B., Mandon-Pépin, B., Stefansdottir, A., Filis, P., Kyle, C., Zhang, Z., Allen, C., Purdie, L., Jouneau, L., Cotinot, C., Rhind, S.M., Sinclair, K.D., Fowler, P.A., 2016. The fetal ovary exhibits temporal sensitivity to a 'real-life' mixture of environmental chemicals. Sci. Rep. 6, 22279. https://doi.org/10.1038/srep22279.

Lea, R.G., Mandon-Pépin, B., Loup, B., Poumerol, E., Jouneau, L., Egbowon, B.F., Bowden, A., Cotinot, C., Purdie, L., Zhang, Z., Fowler, P.A., Sinclair, K.D., 2022. Ovine fetal testis stage-specific sensitivity to environmental chemical mixtures. Reproduction 163, 119–131. https://doi.org/10.1530/REP-21-0235.

Lind, P.M., Gustafsson, M., Hermsen, S.A.B., Larsson, S., Kyle, C.E., Örberg, J., Rhind, S. M., 2009. Exposure to pastures fertilised with sewage sludge disrupts bone tissue homeostasis in sheep. Sci. Total Environ. 407, 2200–2208. https://doi.org/10.1016/j.scitotenv.2008.12.035.

Manimaran, S., Selby, H.M., Okrah, K., Ruberman, C., Leek, J.T., Quackenbush, J., Haibe-Kains, B., Bravo, H.C., Johnson, W.E., 2016. BatchQC: interactive software for evaluating sample and batch effects in genomic data. Bioinformatics 32, 3836–3838. https://doi.org/10.1093/bioinformatics/btw538.

Manna, P.R., Stetson, C.L., Slominski, A.T., Pruitt, K., 2016. Role of the steroidogenic acute regulatory protein in health and disease. Endocrine 51, 7–21. https://doi.org/10.1007/s12020-015-0715-6.

Miyamoto, T., Bando, Y., Koh, E., Tsujimura, A., Miyagawa, Y., Iijima, M., Namiki, M., Shiina, M., Ogata, K., Matsumoto, N., Sengoku, K., 2016. A PLK4 mutation causing azoospermia in a man with Sertoli cell-only syndrome. Andrology 4, 75–81. https://doi.org/10.1111/andr.12113.

Mruk, D.D., Cheng, C.Y., 2015. The mammalian blood-testis barrier: its biology and regulation. Endocr. Rev. 36, 564–591. https://doi.org/10.1210/er.2014-1101.

NAS, 2017. Application of Systematic Review Methods in an Overall Strategy for Evaluating Low-Dose Toxicity from Endocrine Active Chemicals. National Academies Press, Washington, D.C. https://doi.org/10.17226/24758.
Nistal, M., González-Peramato, P., Serrano, Á., 2017. Testicular dysgenesis syndrome (TDS). In: Clues in the Diagnosis of Non-Tumoral Testicular Pathology. Springer International Publishing, Cham, pp. 101–109. https://doi.org/10.1007/978-3-319-49364-0_13.
Palladino, M.A., Pirlamarla, P.R., Mcnamara, J., Sottas, C.M., Korah, N., Hardy, M.P., Hales, D.B., Hermo, L., 2011. Normoxic expression of hypoxia-inducible factor 1 in rat Leydig cells in vivo and in vitro. J. Androl. 32, 307–323. https://doi.org/10.2164/jandrol.110.011494.
Paul, C., Robaire, B., 2013. Impaired function of the blood-testis barrier during aging is preceded by a decline in cell adhesion proteins and GTPases. PLoS One 8, e84354. https://doi.org/10.1371/journal.pone.0084354.
Paul, C., Rhind, S.M., Kyle, C.E., Scott, H., McKinnell, C., Sharpe, R.M., 2005. Cellular and hormonal disruption of fetal testis development in sheep reared on pasture treated with sewage sludge. Environ. Health Perspect. 113, 1580–1587. https://doi.org/10.1289/ehp.8028.
Rhind, S.M., Smith, A., Kyle, C.E., Telfer, G., Martin, G., Duff, E., Mayes, R.W., 2002. Phthalate and alkyl phenol concentrations in soil following applications of inorganic fertiliser or sewage sludge to pasture and potential rates of ingestion by grazing ruminants. J. Environ. Monits 4, 142–148. https://doi.org/10.1039/b107539j.
Rhind, S.M., Kyle, C.E., Telfer, G., Duff, E.I., Smith, A., 2005. Alkyl phenols and diethylhexyl phthalate in tissues of sheep grazing pastures fertilized with sewage sludge or inorganic fertilizer. Environ. Health Perspect. 113, 447–453. https://doi.org/10.1289/ehp.7469.
Rhind, S.M., Kyle, C.E., MacKie, C., McDonald, L., 2009. Accumulation of endocrine disrupting compounds in sheep fetal and maternal liver tissue following exposure to pastures treated with sewage sludge. J. Environ. Monit. 11, 1469–1476. https://doi.org/10.1039/b902085c.
Rhind, S.M., Kyle, C.E., MacKie, C., McDonald, L., Zhang, Z., Duff, E.I., Bellingham, M., Amezaga, M.R., Mandon-Pepin, B., Loup, B., Cotinot, C., Evans, N.P., Sharpe, R.M., Fowler, P.A., 2010. Maternal and fetal tissue accumulation of selected endocrine disrupting compounds (EDCs) following exposure to sewage sludge-treated pastures before or after conception. J. Environ. Monit. 12, 1582–1593. https://doi.org/10.1039/c0em00009d.
Rhind, S.M.M., Kyle, C.E.E., Ruffie, H., Calmettes, E., Osprey, M., Zhang, Z.L.L., Hamilton, D., McKenzie, C., 2013. Short- and long-term temporal changes in soil concentrations of selected endocrine disrupting compounds (EDCs) following single or multiple applications of sewage sludge to pastures. Environ. Pollut. 181, 262–270. https://doi.org/10.1016/j.envpol.2013.06.011.
Rider, C.V., Furr, J., Wilson, V.S., Gray, L.E., 2008. A mixture of seven antiandrogens induces reproductive malformations in rats. Int. J. Androl. 31, 249–262. https://doi.org/10.1111/j.1365-2605.2007.00859.x.
Rodprasert, W., Toppari, J., Virtanen, H.E., 2021. Endocrine disrupting chemicals and reproductive health in boys and men. Front. Endocrinol. (Lausanne). 12, 833–847. https://doi.org/10.3389/fendo.2021.706532.
Sargent, K.M., Clopton, D.T., Lu, N., Pohlmeier, W.E., Cupp, A.S., 2016. VEGFA splicing: divergent isoforms regulate spermatogonial stem cell maintenance. Cell Tissue Res 363, 31–45. https://doi.org/10.1007/s00441-015-2297-2.
Sharpe, R.M., Skakkebaek, N.E., 2008. Testicular dysgenesis syndrome: mechanistic insights and potential new downstream effects. Fertil. Steril. 89, e33–e38. https://doi.org/10.1016/j.fertnstert.2007.12.026.
Skakkebæk, N.E., 2002. Endocrine disrupters and testicular dysgenesis syndrome. Horm. Res. Paediatr. 57 https://doi.org/10.1159/000058100.
Skakkebæk, N.E., Rajpert-De Meyts, E., Main, K.M., 2001. Testicular dysgenesis syndrome: an increasingly common developmental disorder with environmental aspects. Hum. Reprod. 16, 972–978. https://doi.org/10.1093/humrep/16.5.972.
Smith, K., Brown, P., Barr, F., 2012a. A survey of congenital reproductive abnormalities in rams in abattoirs in South West England. Reprod. Domest. Anim. 47, 740–745. https://doi.org/10.1111/j.1439-0531.2011.01952.x.
Smith, K., Brown, P., Barr, F., Parkinson, T., 2012b. Cryptorchidism in sheep: a clinical and abattoir survey in the United Kingdom. Open J. Vet. Med 02, 281–284. https://doi.org/10.4236/ojvm.2012.24044.
Snyder, E., Chukrallah, L., Seltzer, K., Goodwin, L., Braun, R.E., 2020. ADAD1 and ADAD2, testis-specific adenosine deaminase domain-containing proteins, are required for male fertility. Sci. Rep. 10, 11536. https://doi.org/10.1038/s41598-020-67834-5.
Su, W., Wong, E.W.P., Mruk, D.D., Cheng, C.Y., 2012. The scribble/lgl/dlg polarity protein complex is a regulator of blood-testis barrier dynamics and spermatid polarity during spermatogenesis. Endocrinology 153, 6041–6053. https://doi.org/10.1210/en.2012-1670.
Takahashi, N., Davy, P.M.C., Gardner, L.H., Mathews, J., Yamazaki, Y., Allsopp, R.C., 2016. Hypoxia inducible factor 1 alpha is expressed in germ cells throughout the murine life cycle. PLoS One 11, 1–14. https://doi.org/10.1371/journal.pone.0154309.
Tang, S., Wang, X., Li, W., Yang, X., Li, Z., Liu, W., Li, C., Zhu, Z., Wang, L., Wang, Jiaxiong, Zhang, L., Sun, X., Zhi, E., Wang, H., Li, H., Jin, L., Luo, Y., Wang, Jian, Yang, S., Zhang, F., 2017. Biallelic mutations in CFAP43 and CFAP44 cause male infertility with multiple morphological abnormalities of the sperm flagella. Am. J. Hum. Genet. 100, 854–864. https://doi.org/10.1016/j.ajhg.2017.04.012.
Uguz, C., Iscan, M., Togan, İ., 2009. Alkylphenols in the environment and their adverse effects on living organisms. Kocatepe Vet. J. 2, 49–58.
Venkatesan, A.K., Halden, R.U., 2014a. Contribution of polybrominated dibenzo-p-dioxins and dibenzofurans (PBDD/Fs) to the toxic equivalency of dioxin-like compounds in archived biosolids from the U.S. EPA's 2001 national sewage sludge survey. Environ. Sci. Technol. 48, 10843–10849. https://doi.org/10.1021/es503110j.
Venkatesan, A.K., Halden, R.U., 2014b. Wastewater treatment plants as chemical observatories to forecast ecological and human health risks of manmade chemicals. Sci. Rep. 4, 4–10. https://doi.org/10.1038/srep03731.
Wang, L., Bu, T., Li, L., Wu, X., Wong, C.K.C., Perrotta, A., Silvestrini, B., Sun, F., Cheng, C.Y., 2022. Planar cell polarity (PCP) proteins support spermatogenesis through cytoskeletal organization in the testis. Semin. Cell Dev. Biol. 121, 99–113. https://doi.org/10.1016/j.semcdb.2021.04.008.
Wang, X., Zou, Z., Yang, Z., Jiang, S., Lu, Y., Wang, D., Dong, Z., Xu, S., Zhu, L., 2019. HIF 1 inhibits STAR transcription and testosterone synthesis in murine Leydig cells. J. Mol. Endocrinol. 62, 1–13. https://doi.org/10.1530/JME-18-0148.
Xia, M., Huang, R., Sun, Y., Semenza, G.L., Aldred, S.F., Witt, K.L., Inglese, J., Tice, R.R., Austin, C.P., 2009. Identification of chemical compounds that induce HIF-1α activity. Toxicol. Sci. 112, 153–163. https://doi.org/10.1093/toxsci/kfp123.
Yuan, W., Leisner, T.M., McFadden, A.W., Clark, S., Hiller, S., Maeda, N., O'Brien, D.A., Parise, L.V., 2006. CIB1 is essential for mouse spermatogenesis. Mol. Cell. Biol. 26, 8507–8514. https://doi.org/10.1128/MCB.01488-06.
Zhao, S., Fernald, R.D., 2005. Comprehensive algorithm for quantitative real-time polymerase chain reaction. J. Comput. Biol. 12, 1047–1064. https://doi.org/10.1089/cmb.2005.12.1047.